

CONNECTIVITY INDUCED SYNCHRONOUS REGIMES IN ENSEMBLES OF NEURON-LIKE OSCILLATORS

M.A.Komarov and G.V.Osipov

Abstract— We study Hodgkin-Huxley type model of oscillator activity in the neurons of a snail *Helix pomatia*. The multistability in single neuron model is demonstrated. We investigate the synaptic excitatory coupling and the chain of 20 coupled elements. The various synchronous regimes are found. Also we detect the effects of synchronous burst generation and the formation of synchronous clusters.

I. INTRODUCTION

The affects of synchronization and multistability in neural systems is a new and intriguing application of dynamical theory. This affects are variable for the following reasons. First, the neuron itself is a multi-dimensial nonlinear system that is able to demonstrate different activities such as multistability, tonic spiking, regular or chaotic bursting, and complex transient regimes. Second, neural oscillations are usually the result of interaction of many synaptically connected neurons.[1] Therefore it is necessary to consider the effects of synchronization and multistability on neural systems.

II. SINGLE NEURON

In this article we consider Hodgkin-Huxley type model of oscillator activity in the bursting neurons of a snail *Helix pomatia*[2].

A. Equations

The dynamics of the neuron describes by system of eight first-order differential equations. The model includes:

1. The basic equation governing membrane behaviour is

$$-C_m \frac{dV}{dt} = I_{Na(TTX)} + I_{K(TEA)} \quad (1)$$

$$+ I_k + I_{Na} + I_{Na(V)} + I_B + I_{Ca} + I_{Ca-Ca}$$

Here C_m is membrane capacity, V denotes the membrane potential (mV). The right part of the basic equation represents the sum of ionic currents caused by diffusion calcium, potassium, sodium ions through the cell membrane.

2. Slow-wave generating mechanism

$$I_{Na}(V) = g_{Na}^*(V) \frac{1}{1 + \exp(-0.2(V + 45))} (V - V_{Na});$$

$$I_K = g_K^*(V - V_K); I_{Na} = g_{Na}^*(V - V_{Na});$$

$$I_B = g_B^* m_B h_B (V - V_B);$$

$$\frac{dm_b}{dt} = \left(\frac{1}{1 + \exp(0.4(V + 34))} - m_b \right) \frac{1}{0.05} \quad (2)$$

$$\frac{dh_b}{dt} = \left(\frac{1}{1 + \exp(-0.55(V + 43))} - h_b \right) \frac{1}{1.5} \quad (3)$$

3. Spike generating mechanism (the Hodgkin Huxley sodium TTX-sensitive and potassium TEA-sensitive currents)

$$I_{Na(TTX)} = g_{Na(TTX)}^* m^3 h (V - V_{Na});$$

$$I_{K(TEA)} = g_{K(TEA)}^* n^4 h (V - V_K);$$

$$\frac{dm}{dt} = \left(\frac{1}{1 + \exp(-0.4(V + 31))} - m \right) \frac{1}{0.0005} \quad (4)$$

$$\frac{dh}{dt} = \left(\frac{1}{1 + \exp(0.25(V + 45))} - h \right) \frac{1}{0.01} \quad (5)$$

$$\frac{dn}{dt} = \left(\frac{1}{1 + \exp(-0.18(V + 25))} - n \right) \frac{1}{0.015} \quad (6)$$

4. Calcium currents (transient voltage-dependent (I_{Ca}) and stationary [Ca^{2+}]_{in}-inhibited (I_{Ca-Ca}))

$$I_{Ca} = g_{Ca}^* m_{Ca}^2 (V - V_{Ca})$$

$$\frac{dm_{Ca}}{dt} = \left(\frac{1}{1 + \exp(-0.2V)} - m_{Ca} \right) \frac{1}{0.01} \quad (7)$$

$$I_{Ca-Ca} = \frac{1}{1 + \exp(-0.06(V + 45))} \times$$

$$\times \frac{1}{1 + \exp(k_\beta([Ca] - \beta))}$$

5. Intracellular Ca ions, their fast buffering and uptake by Ca stores.

$$\frac{d[Ca]}{dt} = \rho \left(\frac{-I_{Ca}}{2Fv} - k_s [Ca] \right); v = \frac{4\pi R^3}{3} \quad (8)$$

Here g_i is the maximum conductance of channel. V_i is the apparent equilibrium(reversal) potential. $m, h, n, m_b, h_b, m_{Ca}$ is the gating variables, determines the fraction of open channels. $[Ca]$ is $[Ca^{2+}]_{in}$ (mM), F is Faraday number $85,374 C mol^{-1}$; v is the volume of the cell, k_s is the rate constant of intracellular Ca uptake by intracellular stores, ρ is the endogenous Ca buffer capacity.

This work is done at financial support RFBR-NSC, project N 05-02-90567 and RFBR-MF project N 05-02-19815 and RFBR project N 06-02-16596. G.O. and J.K. acknowledges support of EU-Network BioSim, Contract No. LSHB-CT-2004-005137

M.A.Komarov and G.V.Osipov are with Radiophysical department, University of Nizhny Novgorod, Gagarin ave. 23, 603950 Nizhny Novgorod, Russia; makomar@mail.com, osipov@rf.unn.ru

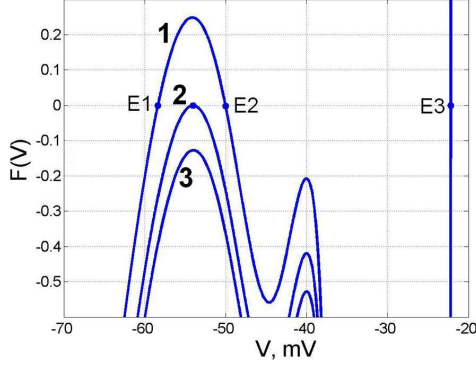


Fig. 1. Graphs of function $F(V)$. Control parameter - g_{Na} . $g_{Na1} = 0.014 \text{ mS}$, $g_{Na2} = 0.01665 \text{ mS}$, $g_{Na3} = 0.018 \text{ mS}$. E1,E2,E3 - points of equilibriums.

B. Steady states and bifurcation to oscillatory regime

First, we are interesting in steady states. Their coordinates can be found from system of equations:

$$\begin{cases} g_{Na}^*(V) \frac{1}{1+\exp(-0.2(V+45))} (V - V_{Na}) + \\ + g_K^*(V - V_K) + g_{Na}^*(V - V_{Na}) + \\ + g_B^* m_B h_B (V - V_B) + g_{Na}^*(TTX) m^3 h (V - V_{Na}) + \\ + g_K^*(TEA) n^4 h (V - V_K) + g_{Ca}^* m_{Ca}^2 (V - V_{Ca}) + \\ + \frac{1}{1+\exp(-0.06(V+45))} \frac{1}{1+\exp(k_\beta([Ca] - \beta))} = 0 \\ \left(\frac{1}{1+\exp(0.4(V+34))} - m_b \right) \frac{1}{0.05} = 0 \\ \left(\frac{1}{1+\exp(-0.55(V+43))} - h_b \right) \frac{1}{1.5} = 0 \\ \left(\frac{1}{1+\exp(-0.4(V+31))} - m \right) \frac{1}{0.0005} = 0 \\ \left(\frac{1}{1+\exp(0.25(V+45))} - h \right) \frac{1}{0.01} = 0 \\ \left(\frac{1}{1+\exp(-0.18(V+25))} - n \right) \frac{1}{0.015} = 0 \\ \left(\frac{1}{1+\exp(-0.2V)} - m_{Ca} \right) \frac{1}{0.01} = 0 \\ \rho \left(\frac{-I_{Ca}}{2Fv} - k_s [Ca] \right) = 0 \end{cases}$$

Using a simple mathematical transformation this system was reduced to one equation only depends on V :

$$F(V) = 0$$

Using numerical analysis of $F(V)$ we can find the zeros of the function and thus the coordinates of equilibriums. Fig 1 represents the graphs of function $F(V)$ plotted of different parameter g_{Na} . Increasing g_{Na} from 0.014 mS to 0.018 mS leads to the change of the dynamics of neuron from excitatory mode to periodic bursting mode.

The first curve (marked by label "1") in Fig. 1 was plotted with $g_{Na} = 0.014 \text{ mS}$. In this case neuron is in excitatory mode and dynamical system have 3 equilibriums: points E1, E2, E3 (zeros of function $F(V)$). For analysis of stability of this equilibrium we have to linearize described above system

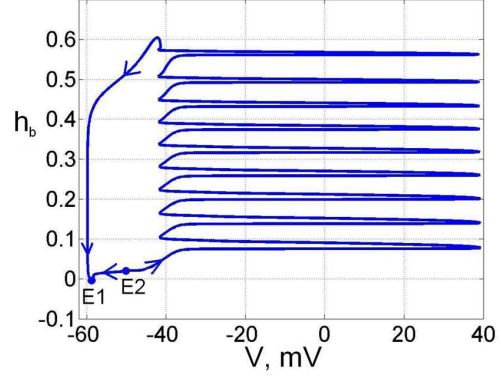


Fig. 2. Phase trajectory and stable states. Plane (h_B, V) ; $g_{Na} = 0.014 \text{ mS}$.

of differential equations in the point of equilibriums:

$$\begin{cases} \frac{dV}{dt} = a_{11}(V - V^*) + a_{12}(m_b - m_b^*) + \\ + a_{13}(h_b - h_b^*) + a_{14}(m - m^*) + a_{15}(h - h^*) + \\ + a_{16}(n - n^*) + a_{17}(m_{Ca} - m_{Ca}^*) + a_{18}(Ca - Ca^*) \\ \frac{dm_b}{dt} = a_{21}(V - V^*) + a_{22}(m_b - m_b^*) \\ \frac{dh_b}{dt} = a_{31}(V - V^*) + a_{33}(h_b - h_b^*) \\ \frac{dm}{dt} = a_{41}(V - V^*) + a_{44}(m - m^*) \\ \frac{dh}{dt} = a_{51}(V - V^*) + a_{55}(h - h^*) \\ \frac{dn}{dt} = a_{61}(V - V^*) + a_{66}(n - n^*) \\ \frac{dm_{Ca}}{dt} = a_{71}(V - V^*) + a_{77}(m_{Ca} - m_{Ca}^*) \\ \frac{d[Ca]}{dt} = a_{81}(V - V^*) + a_{87}(m_{Ca} - m_{Ca}^*) + \\ + a_{88}([Ca] - [Ca]^*) \end{cases}$$

there a_{ij} -coefficients at the linear members of series expansion of functions in right parts of equations (1)-(8) in the point of equilibrium. The real part of eigenvalues of matrix of coefficients a_{ij} for points E1, E3 turn out negative that indicates stability of this states. Calculating eigenvalues for E2 shows unstable behavior of this state. To understand the dynamics of the system and the bifurcation leading to oscillatory regime we plot the projection of phase trajectory which corresponds to excitation of neuron (Fig. 2). Equilibriums E1 and E2 situate on the invariant curve. When the dynamical system is positioned in equilibrium E1 neuron doesn't fire, his action potential doesn't change and equal to potential of a rest. Changing the initial conditions (by adding impulse of depolarizing current for example) leads to the situation when dynamical system leaves the equilibrium and get on invariant curve which corresponds to burst of spikes of action potential. Then dynamical system returns by a curve to an equilibrium again and proceeds to locate in a rest state.

It is necessary to notice that in the case that presented in Fig. 2 phase trajectory did not get into domain of attraction of stable state E3, which have the following coordinates:

$$\begin{aligned} V &= -22.1526 \text{ mV}; m = 0.9718; h = 0.0033; n = 0.6254; \\ m_{Ca} &= 0.0118; m_b = 0.0087; h_b = 1.0; Ca = 0.0 \end{aligned}$$

At $g_{Na} = 0.01665 \text{ mS}$ take place the bifurcation of saddle-node on invariant circle. The fusion of equilibriums E1 and E2 illustrates curve marked by label "2" in Fig. 2.

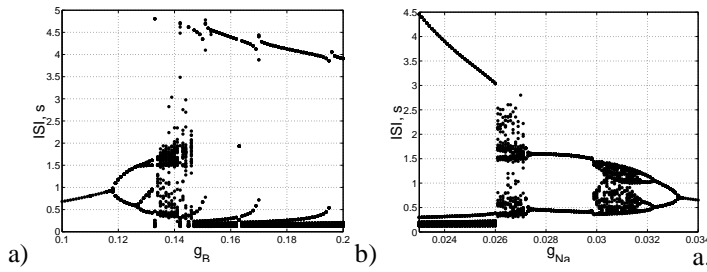


Fig. 3. Bifurcation diagrams. a) Control parameter - $g_B, g_{Na} = 0.0231 mS$. b) Control parameter - $g_{Na}, g_B = 0.16 mS$

Further increasing of g_{Na} leads to disappearing of states E1 and E2 (curve marked by label "3" in Fig.2.) via a bifurcation of saddle-node on invariant circle and appearing of homoclinic orbit corresponding to a periodic bursting mode.

It is very interesting to note that the steady state E3 does not disappears and almost doesn't change own coordinates and behavior in rational range of parameters. Thus dynamics in the single neuron depends not only on parameters and also on initial conditions. Regime when the system locates in the steady state E3 we call "regime of oscillatory death".

Analytical investigation of Komendantov-Kononenko model has shown that:

- the model change own dynamics from excitatory to firing mode via a bifurcation of saddle-node on invariant curve.
- the dynamical system is multistable. Except for attractors corresponding to different oscillatory regimes there is a stable state in the phase space corresponding to regime of oscillatory death, thus behavior of neuron depends on initial conditions.

C. Regimes of activity

In this section we present results of numerical analysis of described above neuron model. Change between different states of electrical activity and the appearance of a chaotic discharge can be evoked by long-lasting alteration of chemosensitive conductances g_B and g_{Na} participating in slow-wave generation [3]. Thus, it is interesting to investigate the interspike intervals (ISI) dependence of the model neuron on both the g_B and g_{Na} conductances as the control parameters. Figure 3 shows the bifurcation diagrams obtained for these parameters.

Bifurcation diagrams show that the model can reproduce various types of activities:

- i) Periodic spiking activity $g_B = 0.1 mS, g_{Na} = 0.0231 mS$ Corresponding time series are showed in Fig. 4a.
- ii) Chaotic spiking activity $g_{Na} = 0.0265 mS, g_B = 0.16 mS$. In this case value of ISI does not remain to constants during the time of realization (Fig. 4b). It is necessary to note, that chaos in the dynamical system results from the cascade of period-doubling bifurcation.

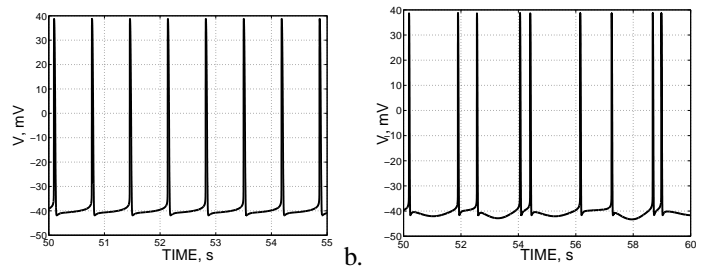


Fig. 4. a. Realization of periodic spiking. $g_B = 0.1 mS, g_{Na} = 0.0231 mS$. b. Realization of irregular activity. $g_{Na} = 0.0265 mS, g_B = 0.16 mS$

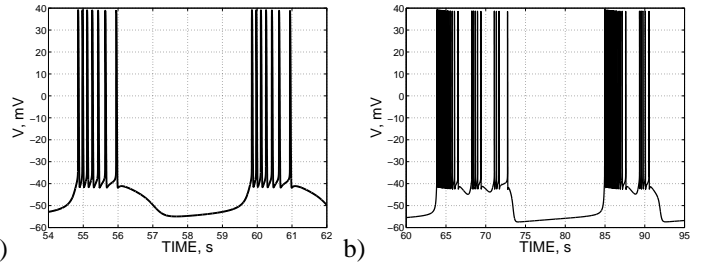


Fig. 5. a) Realization of periodic bursting activity. $g_b = 0.16 mS, g_{Na} = 0.024 mS$. b) Realization of chaotic bursting activity. $g_B = 0.18 mS, g_{Na} = 0.02 mS, g_{Ca-Ca} = 0.01 mS, g_{Na}(V) = 0.13 mS, g_{Ca} = 1.0 mS$

- iii) Periodic bursting activity. $g_B = 0.16 mS, g_{Na} = 0.024 mS$. In Fig. 5a we can see the periodic bursts (series of spikes) with two time scales - big period of time between bursts (dots at the top of the diagram) and small period of time corresponding to ISI of the spikes inside of bursts (dots at the bottom of the diagram).
- iv) Chaotic bursting activity $g_B = 0.18 mS, g_{Na} = 0.02 mS, g_{Ca-Ca} = 0.01 mS, g_{Na}(V) = 0.13 mS, g_{Ca} = 1.0 mS$ Other parameters were not changed. Corresponding time series are represented in Fig. 5b.
- v) Regime of oscillatory death. The analytical investigation of this model has shown that the dynamical system is multistable. Except for attractors corresponding to different oscillatory regimes there is a steady state in the phase space which corresponds to nonoscillatory mode.

Therefore, large dimension of phase space and number of control parameters lead to a wide set of regimes and multistability.

III. CHAIN OF NEURONS

In this section we present results of our study of collective behavior in the chain of 20 elements of synaptic excitatory coupling. Excitatory coupling is modeled by synaptic current $I_{syn} = d_{syn} r(t) (E_{syn} - V_{post})$ [4]. Here d_{syn} (further d) is a maximum conductance of the channel, $E_{syn} = 0 mV$ is the reversal potential. The share of the open channels $r(t)$

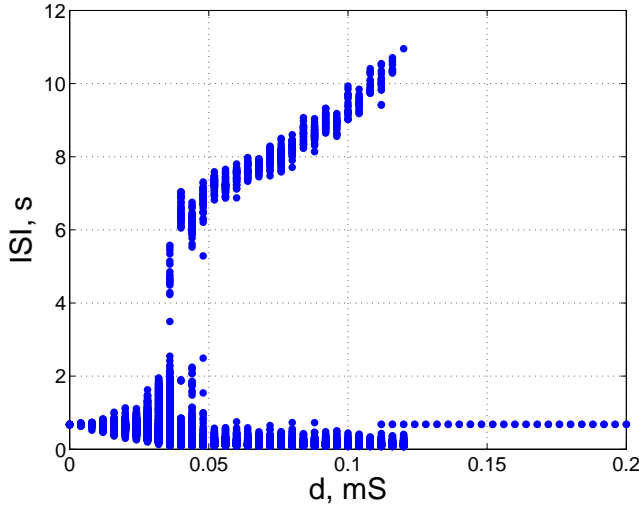


Fig. 6. Bifurcation diagram. Chain of 20 periodic spiking elements. Parameters: $g_B = 0.1 \text{ mS}$, $g_{N\alpha} = 0.0231 \text{ mS}$

in a synapse was set by the standard kinetic equation:

$$\frac{dr}{dt} = \alpha_s A(1 - r) - \beta_s r;$$

Here $\alpha_s = 500 \text{ s}^{-1}$; $\beta_s = 20 \text{ s}^{-1}$; $A = 0.5$ during 2 ms after a spike and $A = 0$ otherwise. In this series of experiments d becomes the one of control parameters. The primary intent is a investigation of various aspects of interaction of the coupling neurons such as phase and out of phase synchronization, transition to a new modes, multistability and others. A depolarizing current $I_{ext} \in [0.0; 0.02] \text{ nA}$ (taken randomly) was added to the basic equation to bring small distinction between neurons. The time series are presented in the spatio-temporal diagrams.

A. Periodic spiking

First we consider periodically spiking neurons. In Fig. 6 is represented dependence of ISIs of each neuron on value of coupling strength. The diagram was created with the step $\Delta d = 0.004 \text{ mS}$. For each value of d was calculated time series during 300 s, first 50 s were not taking into account to reject a transient periods. Initial conditions for each realization did not vary.

There are several areas in Fig. 6 which corresponds to different activities of the neurons:

- i) $d \in (0.0; 0.047] \text{ mS}$ - the region of irregular behavior. Time series are showed in Fig. 7a. There we can see the areas of temporary synchronous bursts. It is an important case of synchronization which have a transient character.
- ii) $d \in (0.047; 0.124] \text{ mS}$ - region of synchronous burst generation. Coupling of neurons leads to an interesting effect: the chain of elements which initially were in periodic spiking mode transform

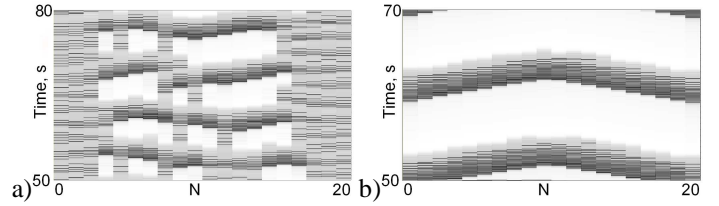


Fig. 7. Spatio-temporal diagrams in the chain. a) Irregular activity and regions of transient burst synchronization. b) Synchronous burst generation. Parameters: $g_B = 0.1 \text{ mS}$, $g_{N\alpha} = 0.0231 \text{ mS}$, a) $d = 0.038 \text{ mS}$, b) $d = 0.06 \text{ mS}$

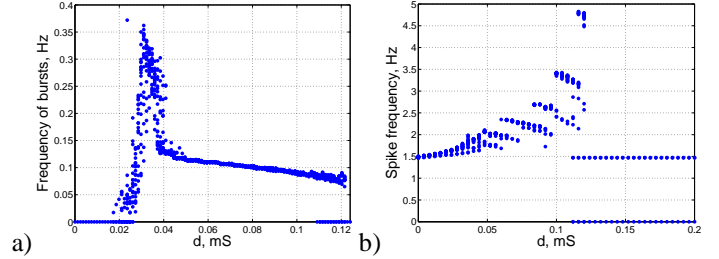


Fig. 8. Dependence frequency of a) Bursts b) Spikes on d . Parameters: $g_B = 0.1 \text{ mS}$, $g_{N\alpha} = 0.0231 \text{ mS}$

their dynamics to periodic bursting mode as a result of interaction. Time series is presented in Fig. 7b. The process of burst synchronization is represented in fig. 8a. The increasing d first guide to synchronization and then to desynchronization of bursts with the decreasing burst frequency. The spikes inside of bursts show more complex dynamics. With increasing of d increases the burst duration and number of spikes in bursts. The adding of spikes in bursts of different elements takes place at different values of d . Thus the number of spikes differs and the equalization of spike frequencies does not occur.

- iii) $d > 0.116 \text{ mS}$ - the desynchronization of bursts precedes to the regime when some neurons stop firing as a result of interaction in a chain. Corresponding time series are presented in Fig. 9. Thus there becomes apparent an effect of oscillatory death described in section II. This mode leads to formation of clusters of chaotic spiking, periodic bursting and oscillatory death elements. The size of formed cluster determines the behavior of elements

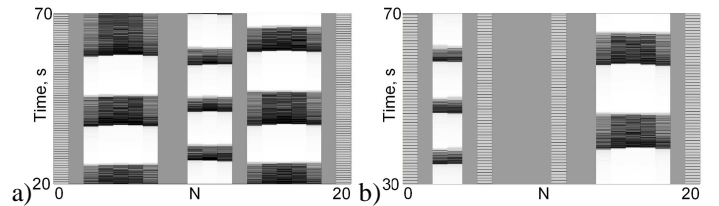


Fig. 9. Cluster formation through the effect of oscillatory death. Parameters: $g_B = 0.1 \text{ mS}$, $g_{N\alpha} = 0.0231 \text{ mS}$, a) $d = 0.12248 \text{ mS}$, b) $d = 0.1225 \text{ mS}$

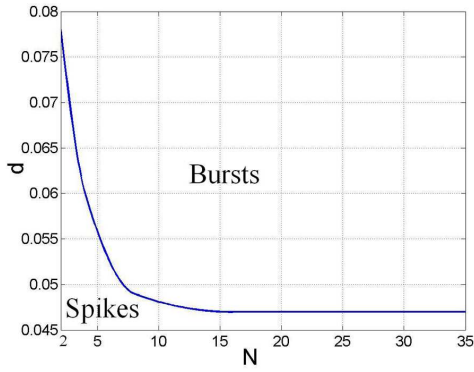


Fig. 10. Dependence type of behavior on coupling strength and size of cluster. Parameters: $g_B = 0.1 \text{ mS}$, $g_{Na} = 0.0231 \text{ mS}$

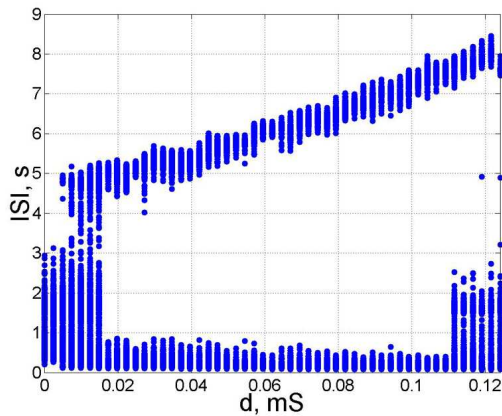


Fig. 11. Bifurcation diagram of chaotic elements. Parameters: $g_B = 0.137 \text{ mS}$, $g_{Na} = 0.0231 \text{ mS}$

inside of it. Such scaling dependence represents in Fig. 10. It shows the dependence of threshold value of d when behavior of cluster changes to clear synchronous bursts without any chaotic discharges upon size of cluster (N). It is necessary to notice that clusters doesn't interact through the neurons in oscillatory death mode.

B. Chaotic neurons

The dependence of behavior in the chain is presented in Fig. 11. The regime of collective synchronous burst generation occurs through the formation of clusters of bursting elements. This effect is presented in Fig. 12a and it is the main difference between chain of periodically and chaotically spiking elements.

As in a previous case there is an effect of cluster formation through the oscillatory death elements at a value of $d > 0.116 \text{ mS}$. Corresponding time series is represented in Fig. 12b There are clusters of oscillatory death, periodically bursting and as against to previous case chaotically spiking elements.

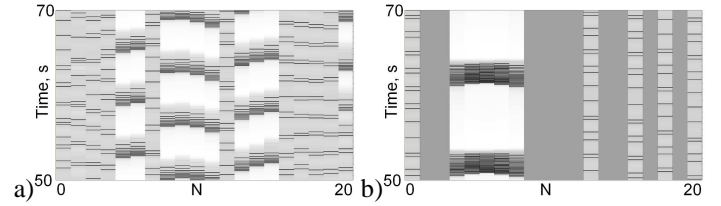


Fig. 12. Spatio-temporal diagram of a chain. a) Clusters of bursts precedes the collective burst generation. b) Clusters of oscillatory silent, periodically bursting and chaotically spiking elements. Parameters: $g_B = 0.137 \text{ mS}$, $g_{Na} = 0.0231 \text{ mS}$, a) $d = 0.01 \text{ mS}$, b) $d = 0.1233 \text{ mS}$

IV. CONCLUSIONS

The analytical investigation of Komendantov-Kononenko model has shown that except for attractors corresponding to different oscillatory regimes there a stable state in the phase space that corresponds to mode of oscillatory death. This leads to the multistability of single neuron and as well in the chain of elements and also to effect of formation of clusters of oscillating and death elements in the chain.

The effect of collective burst generation by a chain of initially spiking elements is detected. In the case of periodic elements the regime of transient burst synchronization precedes to a regime of collective synchronous burst generation. In the case of chaotic elements the increasing of coupling strength first leads to the generation of bursts in some clusters of elements and then to a the collective synchronous burst generation.

REFERENCES

- [1] M. Rabinovich. *Neural synchronization: Peculiarity and Generality*, Invited Talk - SynCoNet2007 (2007).
- [2] Komendantov. A, Kononenko. N *Deterministic chaos in mathematical model of pacemaker activity in bursting neurons of snail, Helix Pomatia.*, J. Theor. biol. (1996) 183,219-230.
- [3] Kononenko. N, J. Theor. biol. (1994).
- [4] A. Destexhe, Z. F. Mainen, T. J. Sejnowski *Journal of Computational Neuroscience*. 1, 195-230, (1994)